STM JOURNALS

Journal of Power Electronics & Power Systems
ISSN: 2249-863X(online), ISSN: 2321-4244(print)
Volume 6, Issue 1
www.stmjournals.com

Speed Estimation of High-Speed Hysteresis Motor Based on Extended Kalman Filter

AH. Niasar**, AN. Darbaghshahi, M. Shirani
Department of Electrical and Computer Engineering, University of Kashan, Kashan, Iran

Abstract

High-speed hysteresis motors are used in special industries such as medical centrifuges and gyroscopes. In spite of that, they are synchronous motors in some situations they may work in asynchronous speed. So, for reliable performance of hysteresis motor, closed loop control strategies are employed. On this way, speed/position of rotor must be known. Due to difficulty of using the speed sensors in high-speed hysteresis motor drives, employing the speed estimation and sensorless control techniques are more valuable. On the other hand, dynamic model of hysteresis motor is more complicated than other motors due to nonlinear characteristics of rotor's material. So, to estimate the state variables of nonlinear and uncertain model of hysteresis motor, this paper uses extended kalman filter as a powerful and robust estimator to gain the rotor speed and flux. The satisfied simulation results confirm that proposed extended kalman filter estimates the rotor speed and rotor flux accurately and it has good static and dynamic performance.

Index Terms: *Extended kalman filter, high speed, hysteresis motor, sensorless, speed estimation, observer, drive*

****Author for Correspondence*** E-mail**:** halvaei@kashanu.ac.ir

INTRODUCTION

Hysteresis motors are brushless synchronous motors which are being used widely in high-speeds applications due to interesting features [1]. Noiseless operation of hysteresis motor is its main advantage because it has no teeth, saliency or winding on the rotor. So, it develops very smooth torque that is a critical point in high speed applications. hysteresis motor like to squirrel-cage induction motor has simple structure. Figure 1 shows a cross section of a hysteresis motor. Its stator is considered to have three-phase two-pole with sinusoidal distributed winding. The rotor comprises of two main parts: (i) magnetic ring which is the basic element for torque providing, (ii) inside part of the rotor that is made of non-magnetic material that acts as a support for the magnetic ring. However, in comparison with other types of motors, hysteresis motors have lower efficiency as high as 75% and low power factor less than 0.5 [2].

Basically, hysteresis motor is a self-starting synchronous motor and it seems that there is no need to rotor's speed and position information or even closed-loop control strategies [3]. However, in some cases such as short time over-load conditions or short failure in power supply, the motor may work at asynchronous conditions. If the over load or failure duration takes long, the slip reaches to a certain value and motor may intend to instability. In these cases, the current speed of the rotor should be available. On the other hand, hysteresis motors are mostly used in variable speed applications and to gain the reliable performance and fast dynamic response, closed-loop strategies such as V/f and FOC [4–6] are employed. Due to the above mentioned reasons physical sensors must be used to identify the rotor speed. But, they are costly and also reduce the reliability of the control system. Moreover, in some cases the rotor rotates in the vacuum and installation of position/speed sensor is impossible. Therefore, using a speed estimator is more convenient.

Most of conventional speed estimators used for electrical motors is based on dynamic model of the motor [7]. Accurate model of motors are essential for successful speed

estimation. Hysteresis motor has got the most complicated dynamic model among all electrical motors due to nonlinear property of B-H curve in rotor's material. Moreover, B-H curve of the rotor varies as well as the varying of the voltage or load [8]. The hysteresis loops of the material used in the rotor and their influences on the parameters of the equivalent circuit are necessary to be taken into consideration adequately. It is demonstrated that some of the equivalent circuit parameters vary significantly with input voltage variation and other operating conditions. So, a nonlinear and robust speed estimator should be employed for hysteresis motor.

According to the system identification theory, the best way to estimate nonlinear system state such as induction motor and permanent magnet synchronous motor drives is the extended kalman filter (EKF) [8, 9]. In this paper, extended kalman filter is used for rotor flux and speed estimation of hysteresis motor. This algorithm establishes a new state equation. The state variables are the stator current and rotor flux, and the input variables are stator voltages. Finally, EKF's results on speed estimation are compared to MRAS's result to show the prominence of EKF method.

MODELING OF HYSTERESIS MOTOR

It is well-known that the outcome of the rotor magnetic material is to create a 'hysteresis lag angle' between the stator MMF and the resultant air-gap flux density waveforms. The lag angle is self-governing of the frequency of rotor magnetization but be in contingent on the zone of the hysteresis loop. The hysteresis motor can operate in both synchronous and sub-synchronous modes. At synchronous speed the fundamental eddy current torque is zero and the operation of the motor is accomplished exclusively by the hysteresis torque. This hysteresis torque is developed by a force between the stator field and the magnetic poles established in the hysteresis ring. However, at any speed except the synchronous one, the motor torque is due to both the hysteresis and eddy current effects. The difference between the model of hysteresis and general synchronous motors comes from the modeling of rotor material that for the hysteresis motor is so different [10].

For the analysis of hysteresis motor and developing an analytical model, B-H loop of rotor's material should be modeled with electrical circuits. On this way, B-H loop hysteresis material of the rotor can be represented by an elliptical curve. It has some advantages rather than rectangular and parallelogram approximations. Figure 2 shows general steady-state equivalent circuit of hysteresis motor in asynchronous and synchronous modes [11]. In these models, parasitic losses and core losses are neglected. In synchronous mode, the source voltage E_h is the voltage induced by the residual magnetism in the hysteresis material and its value is related to the value of the maximum stator current I_s which occurs during starting of the motor [2, 10].

At sub-synchronous mode, hysteresis power can be represented as hysteresis resistance R_h that may be approximated for a circumferential-flux type motor from the power loss approach as (Eqs. 1–4):

$$R_h = \frac{E_g^2}{P_h} = \frac{m\omega\left(K_w N_{ph}\right)^2 \mu V_r}{\pi^2 r_h^2} \sin\beta \tag{1}$$

The lag angle β is delay between stator MMF and air-gap flux density waveforms. For wider B-H loops, β is greater. The representation of the rotor eddy current is carried out by equivalent resistance R_e as:

$$R_e = \frac{12\rho l_h}{10^4 A_h} \tag{2}$$

With elliptical approximation of B-H loop, the reactance due to lag angle caused by hysteresis material and air-gap (magnetizing) reactance can be expressed by:

$$X_h = \omega L_h = \frac{m\omega\left(K_w N_{ph}\right)^2 \mu V_r}{\pi^2 r_h^2} \cos\beta \tag{3}$$

$$X_m = \omega L_m = \frac{2m\omega\left(K_w N_{ph}\right)^2 \mu_0 r_g l_h}{\pi p^2 g_e} \tag{4}$$

For transient performance prediction of hysteresis motor, dynamic model is essential. Contrary to IMs and PMSMs, modeling of hysteresis motor is more complicated due to nonlinear of B-H curve of rotor's material.

There are few contributions for modeling of hysteresis motors in the literature [12–16]. Some of proposed dynamic models have lacks that cannot satisfy the characteristics of hysteresis motors.

In this paper a time-varying dynamic model proposed in is used for estimation of rotor's speed [16]. Figure 3 shows the dynamic model of hysteresis motor in synchronously rotating d-q reference frame. This model is similar to PMSM's model with difference that, in PMSM a flux source (or a voltage source) is considered on d-axis, but in hysteresis motor's model, two voltage sources that are induced by the residual magnetism in the hysteresis material, are considered. Moreover, this model is similar to squirrel-cage induction motor's one, with difference that for IM, the input voltages on rotor d-q axis are considered zero. The stator and rotor voltage equations in rotating d-q reference frame are represented by (Eqs. 5–10):

$$\begin{cases} v_{qs} = r_s i_{qs} + \omega_r \lambda_{ds} + \dfrac{d\lambda_{qs}}{dt} \\ v_{ds} = r_s i_{ds} - \omega_r \lambda_{qs} + \dfrac{d\lambda_{ds}}{dt} \end{cases} \quad \begin{cases} v'_{qr} = r'_r i'_{qr} + \dfrac{d\lambda'_{qr}}{dt} \\ v'_{dr} = r'_r i'_{dr} + \dfrac{d\lambda'_{dr}}{dt} \end{cases} \tag{5}$$

The rotor's parameters in Figure 3 are calculated from:

$$x'_{lr} = \omega L'_{lr} = X_h \tag{6}$$

$$r'_r = R_h \,\|\, \frac{R_e}{s} \tag{7}$$

The input voltages of the rotor in Figure 3 are computed from induced voltage E_h [15, 16]. The linkage flux equations are as:

$$\begin{bmatrix} \lambda_{qs} \\ \lambda_{ds} \\ \lambda'_{qr} \\ \lambda'_{dr} \end{bmatrix} = \begin{bmatrix} L_{ls}+L_m & 0 & L_m & 0 \\ 0 & L_{ls}+L_m & 0 & L_m \\ L_m & 0 & L'_{lr}+L_m & 0 \\ 0 & L_m & 0 & L'_{lr}+L_m \end{bmatrix} \times \begin{bmatrix} i_{qs} \\ i_{ds} \\ i'_{qr} \\ i'_{dr} \end{bmatrix} \tag{8}$$

Finally, electromagnetic torque and rotor speed are obtained from:

$$T_{em} = \frac{3}{2}\frac{P}{2}(\lambda_{ds} i_{qs} - \lambda_{qs} i_{ds}) \tag{9}$$

$$T_{em} - T_{mech} = \frac{2J}{p}\frac{d\omega_r(t)}{dt} \tag{10}$$

The definitions of some symbols, for employed hysteresis motor are listed in Table I.

Speed Estimator Based On Extended Kalman Filter

The kalman filter is a special kind of observer that provides optimal filtering of process and measurement noises if the covariances of these noises are known. For linear systems subject to gaussian measurement or process noise the kalman filter is the optimal state estimator, since it results in minimization of the trace of the estimation error's covariance matrix. For nonlinear systems, subject to gaussian noise one can use the generalization of the kalman filter as formulated in terms of the extended kalman filter (EKF). The state-space equations of EKF can be derived from dynamic model of a hysteresis motor in d-q reference frame as [17, 18]:

$$\begin{bmatrix} \dot{i}_{ds} \\ \dot{i}_{qs} \\ \omega_r \dot{\lambda}'_{dr} \\ \omega_r \dot{\lambda}'_{qr} \end{bmatrix} = \begin{bmatrix} a & 0 & b & c \\ 0 & a & -c & b \\ d & 0 & -\tau_r^{-1} & -\omega \\ 0 & d & \omega & -\tau_r^{-1} \end{bmatrix} \times \begin{bmatrix} i_{ds} \\ i_{qs} \\ \omega_r \lambda'_{dr} \\ \omega_r \lambda'_{qr} \end{bmatrix} + \begin{bmatrix} L_s'^{-1} & 0 \\ 0 & L_s'^{-1} \\ 0 & 0 \\ 0 & 0 \end{bmatrix} \times \begin{bmatrix} v_{ds} \\ v_{qs} \end{bmatrix} \tag{11}$$

Stator currents ate considered as output of EKF. So, the output vector (y) of EKF can be considered as:

$$y = \begin{bmatrix} i_{ds} & i_{qs} \end{bmatrix}^T = C\,x^T(t) = \begin{bmatrix} 1 & 0 & 0 & 0 \\ 0 & 1 & 0 & 0 \end{bmatrix} \times \begin{bmatrix} i_{ds} & i_{qs} & \omega_r \lambda'_{dr} & \omega_r \lambda'_{qr} \end{bmatrix}^T \tag{12}$$

Where, the state vector is defined as:

$$x(t) = \begin{bmatrix} i_{ds}(t) & i_{qs}(t) & \omega_r \lambda'_{dr}(t) & \omega_r \lambda'_{qr}(t) \end{bmatrix}^T \tag{13}$$

The electrical parameters τ_r, L'_s, L_m, R_s and ω_r in Eq. 12 represent the rotor time constant, stator transient inductance, mutual inductance, stator resistance and rotor speed respectively. The other parameters of Eq. 11, are given by:

$$a = -L_s'^{-1}(R_s + L_M \tau_r^{-1}) \quad b = -L_s'^{-1}\tau_r^{-1} \quad c = \omega_r L_s'^{-1} \quad d = L_M \tau^{-1}{}_r \tag{14}$$

The state-space model Eqs. 11 and 12 are the type of model structure used for speed estimation using full order EKF. Supposing these equations as standard state space representation with:

$$\begin{cases} \dot{x}(t) = Ax(t) + Bu(t) \\ y(t) = Cx(t) \end{cases} \quad (15)$$

It is discretized directly using the following relationship [9]:

$$\begin{cases} A_d = I + AT_s + \frac{A^2T_s^2}{2!} + \frac{A^3T_s^3}{3!} + \ldots \\ B_d = BT_s + \frac{ABT_s^2}{2!} + \frac{A^2BT_s^3}{3!} + \ldots \end{cases} \quad (16)$$

Furthermore, the state vector Eq. 19 is extended to rotor speed as follows:

$$x_e(k) = \left[i_{ds}(k) \quad i_{qs}(k) \quad \omega_r \lambda'_{dr}(k) \quad \omega_r \lambda'_{qr}(k) \quad \omega_r(k) \right]^T \quad (17)$$

It is assumed that the real speed varies like a random walk, according to Eq. 20:

$$\omega_r(k+1) = \omega_r(k) + \nu(k) \quad (18)$$

The state noise vector ν(k) represents the error caused from motor parameter variations and discretization. This noise vector can be demonstrated below :

$$\mathrm{cov}(\nu) = E\{\nu\nu^T\} = Q \quad (19)$$

Where, $E\{\nu\nu^i\}$ represent the mathematical expectation. Although with different dynamics, the state variables have approximately the same magnitude and the tuning of the diagonal elements of the system covariance matrix become similar. Moreover, since the two components of the rotor flux have the same magnitude and dynamics, only two elements of the system covariance matrix (Q) must be tuned:

$$Q = \mathrm{diag}([Q_{11} \; Q_{22} \; Q_{33}], 0)$$
$$Q_{33} \approx Q_{22} = Q_{11} \quad (20)$$

Considering the discrete output matrix C_d=C, and applying an approximation of Eqs. 11–16, a 5th order nonlinear state-space model is obtained. Then the denominated full order EKF can be used normally the approximation to the linear terms of Eq. 16 is used, which is acceptable if the sampling time T_s is small enough. This procedure is similar to compute the derivative in Eq. 11 by means of the well-known Euler's formula.

SIMULATION RESULTS

The dynamic model block diagram of hysteresis motor and employed EKF are shown in Figures 4 and 5. Motor parameters used for simulation are listed in Table I. As shown in Figure 5 the inputs of the extended Kalman filter are v_{qs}, v_{ds}. Figure 6 shows the estimated and real speed of the motor. The estimation is accurately carried out via extended Kalman filter at full load condition.

Table I: *Rated Specifications And Parameters Of Used Circumferential-Flux Hysteresis Motor.*

Symbol	Quantity	Value	Dimension
V_{rated}	line rated voltage	380	V
T_{rated}	rated torque	0.01	N.m
f_{rated}	rated frequency	1000	Hz
ω	supply angular frequency	60×1000	rpm
m	number of phase	3	
P	number of poles	2	
J	shaft inertia moment	3×10^{-4}	kg.m^2
R_s	stator resistance	60	Ω/ph
R_c	stator core loss equivalent resistance	10580	Ω/ph
R_h	rated rotor hysteresis resistance	173	Ω/ph
R_e	eddy current resistance of rotor	223	Ω/ph
X_{ls}	stator leakage reactance	78	Ω/ph
X_m	rated magnetizing reactance	165	Ω/ph
X_h	rated rotor hysteresis reactance	195	Ω/ph
l_h	axial length of hysteresis ring	25	mm
g	air gap length	1	mm
t_r	thickness of hysteresis ring	1	mm
β	hysteresis lag angle	42	deg

Moreover, Figures 7–10 show the real and estimated of variable states such as currents and rotor flux components. The real values of variables are tracked with corresponding estimated value.

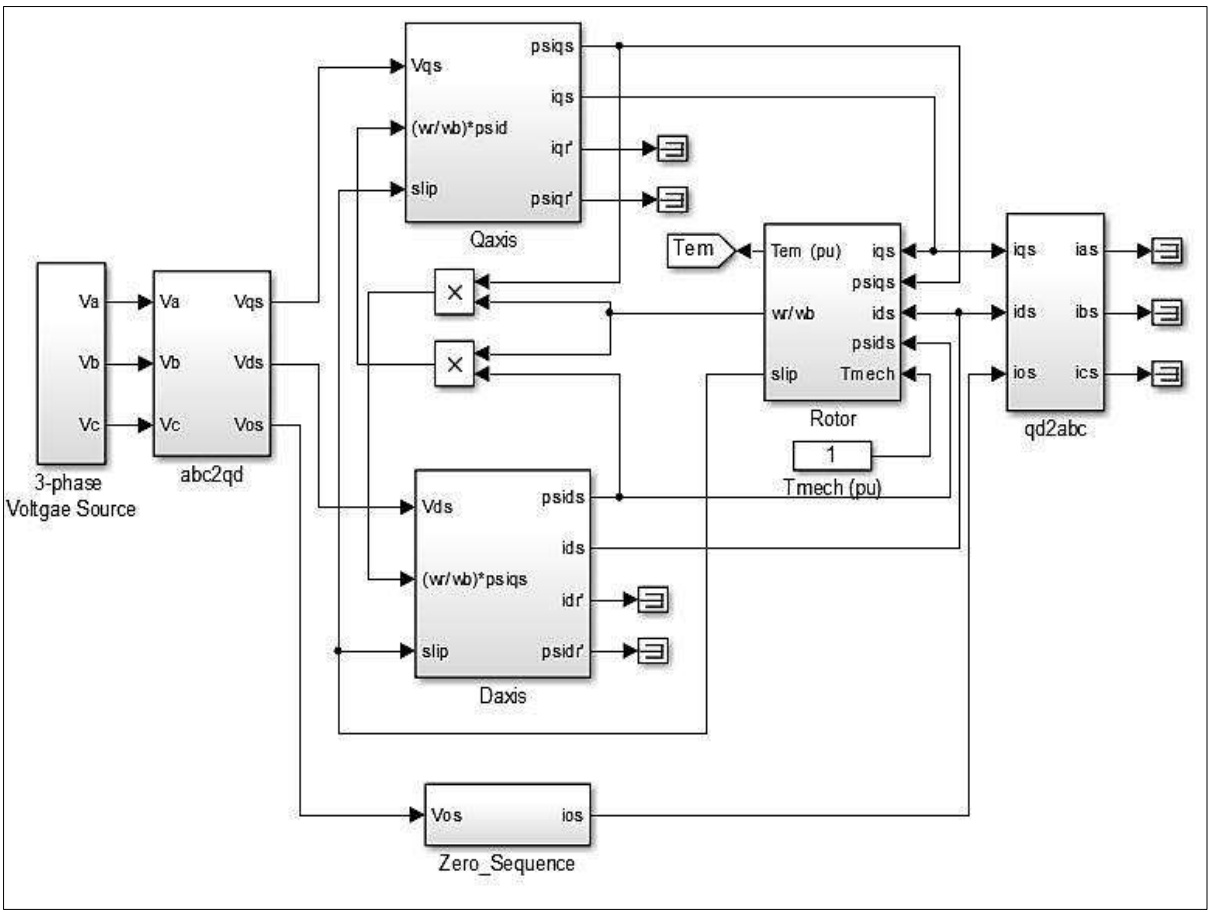

Fig. 4: *Implementation of Dynamic Model Hysteresis Motor in Simulink.*

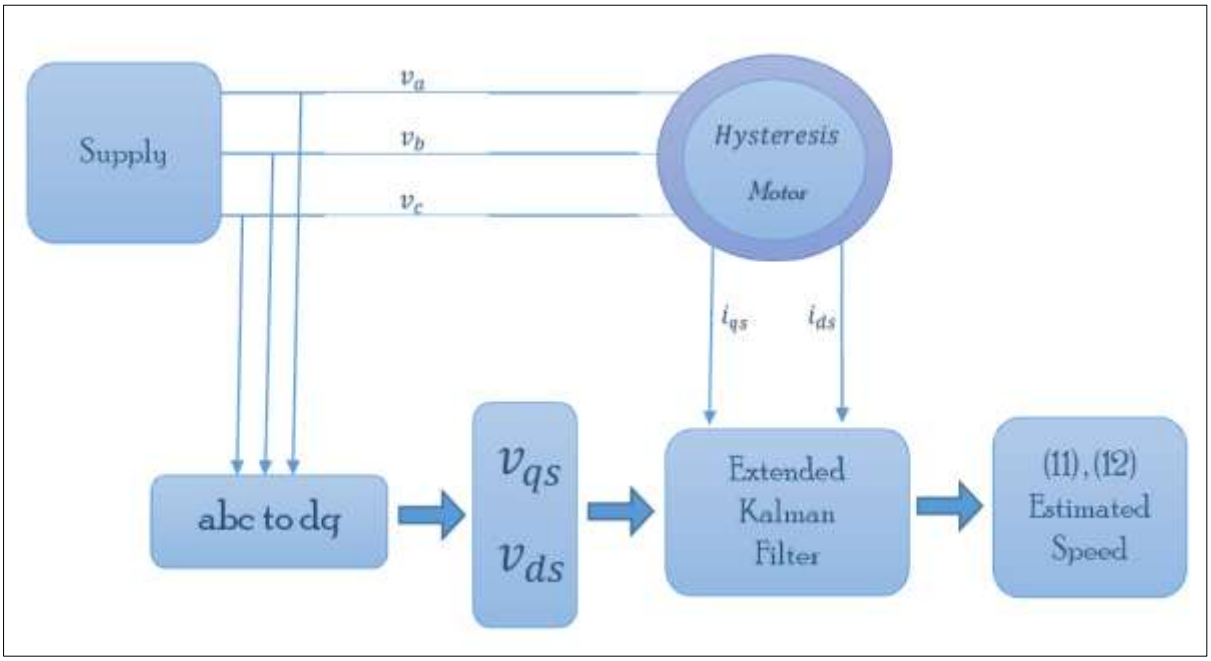

Fig. 5: *Block Diagram of The Proposed EKF.*

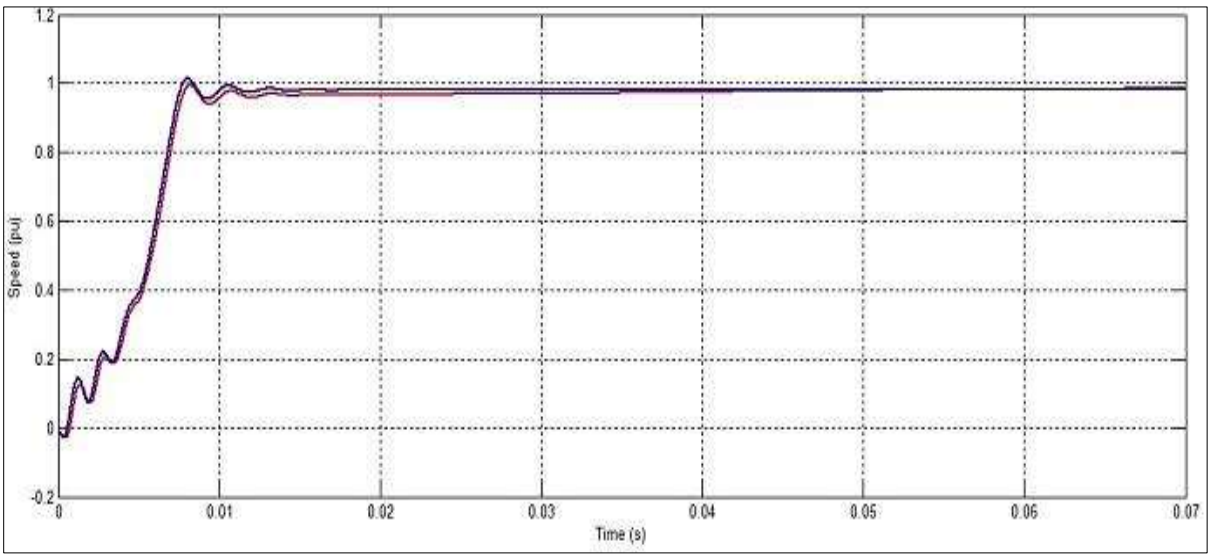

Fig. 6: *Real Speed (Blue) and Estimated Speed (Red) at Full Load Condition.*

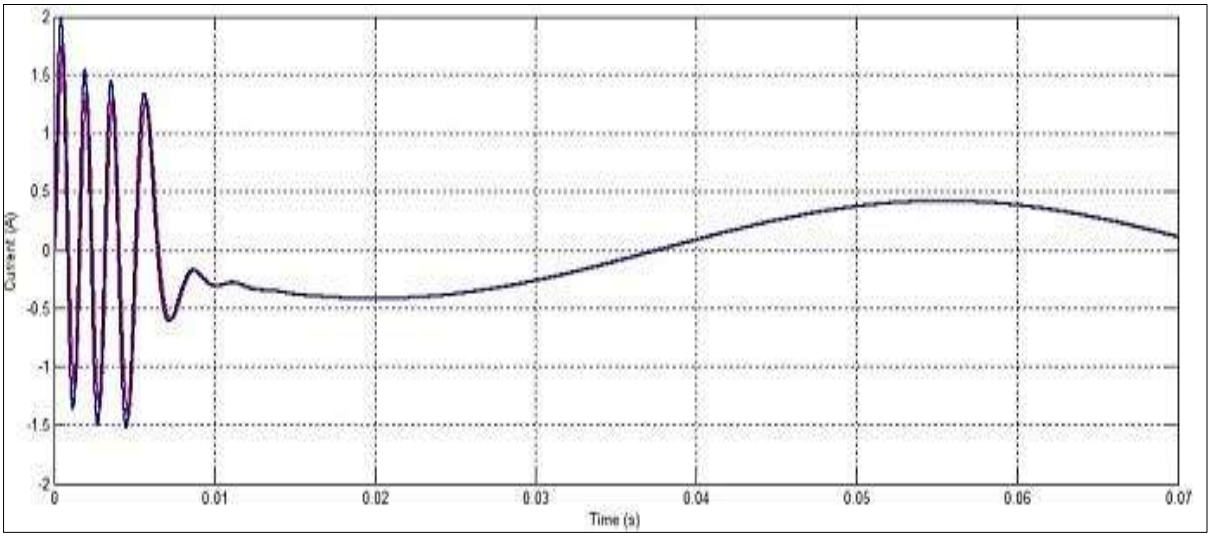

Fig. 7: *Estimated (Red) and Real (Blue)* i_{qs} *(A) at Full Load Condition.*

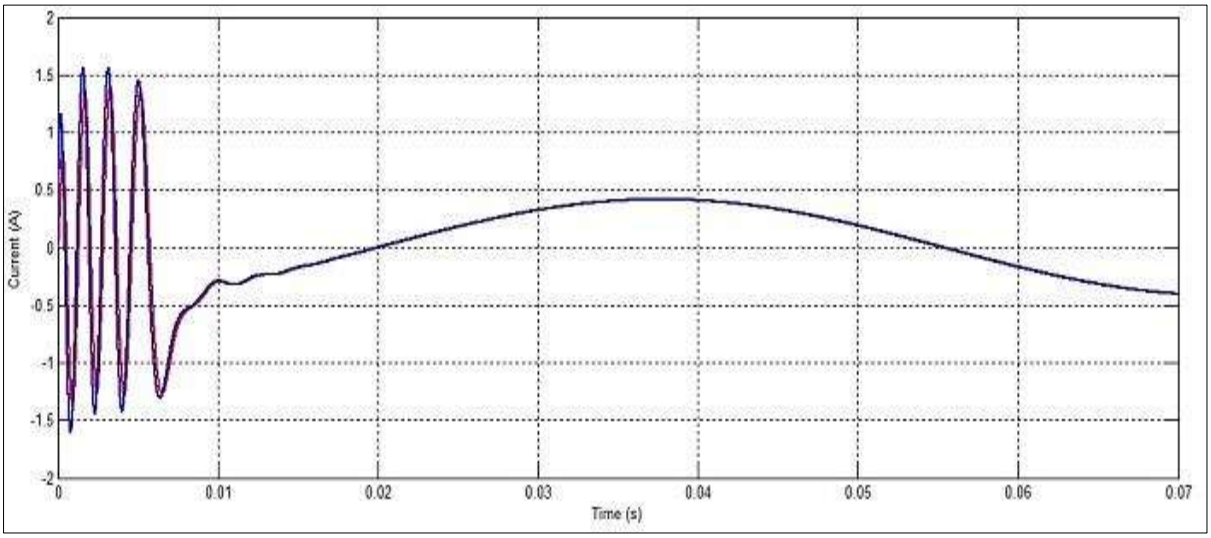

Fig. 8: *Estimated (Red) and Real (Blue)* i_{ds} *(A) at Full Load Condition.*

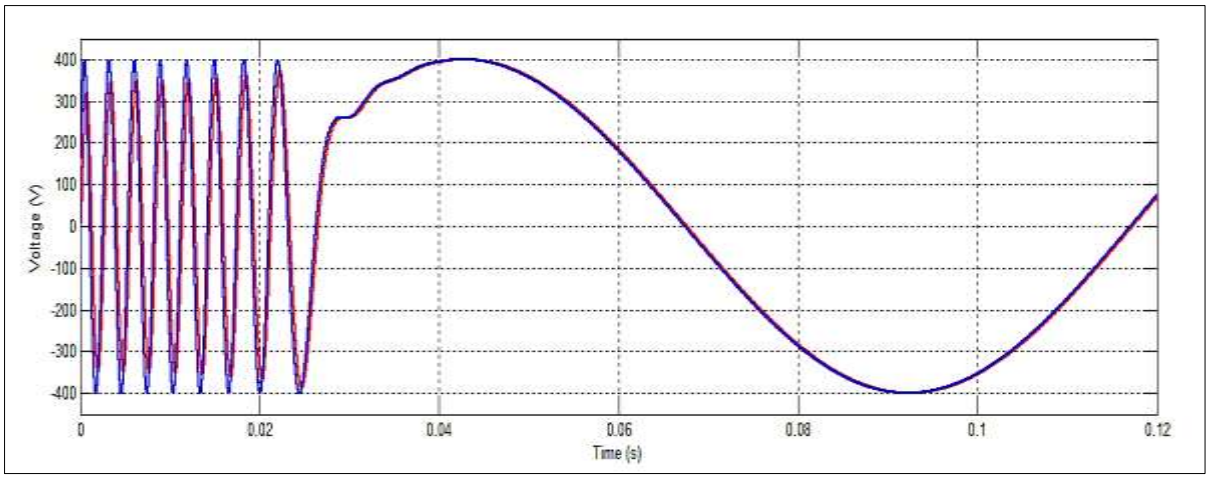

Fig. 9. *Estimated (Red) and Real (Blue)* λ'_{qr} *(Wb) at Full Load Condition.*

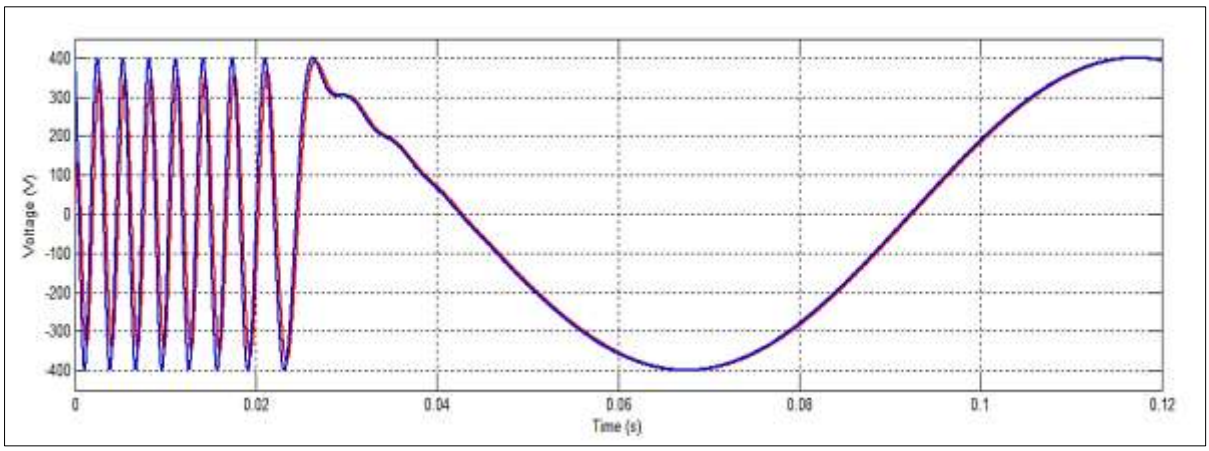

Fig. 10: *Estimated (Red) and Real (Blue)* λ'_{dr} *(Wb) at Full Load Condition.*

For studying the capability of proposed EKF, torque load of hysteresis motor changes suddenly. It changes from 1 pu to 0 at 0.023 sec and 0–0.5 pu at 0.04 sec. The simulation results are shown in Figures 11–15. The speed estimation and state variable estimation is well in transient and steady-state conditions.

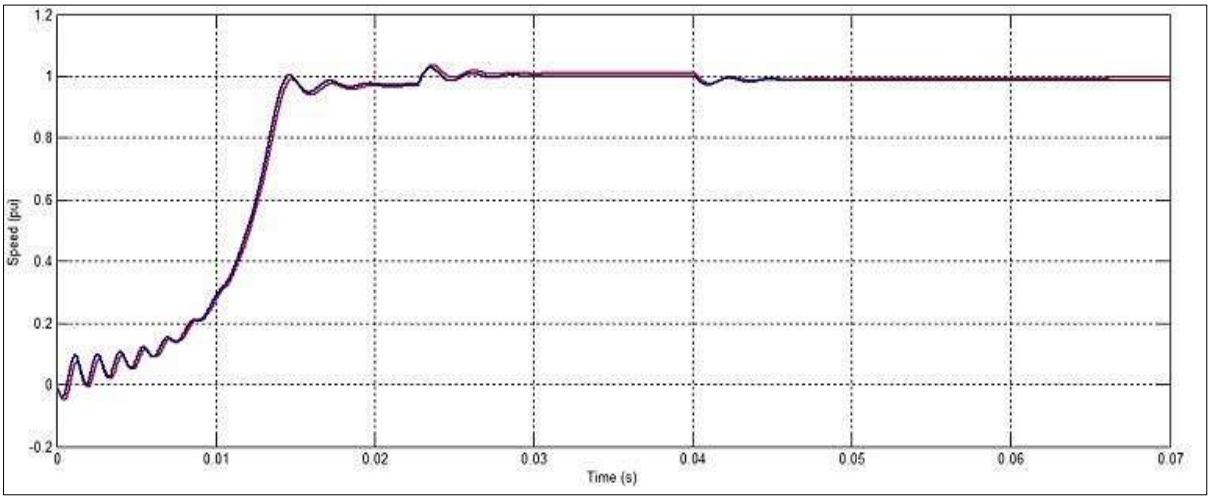

Fig. 11: *Estimated Speed (Red) and Real Speed (Blue) Under Variable Load Condition.*

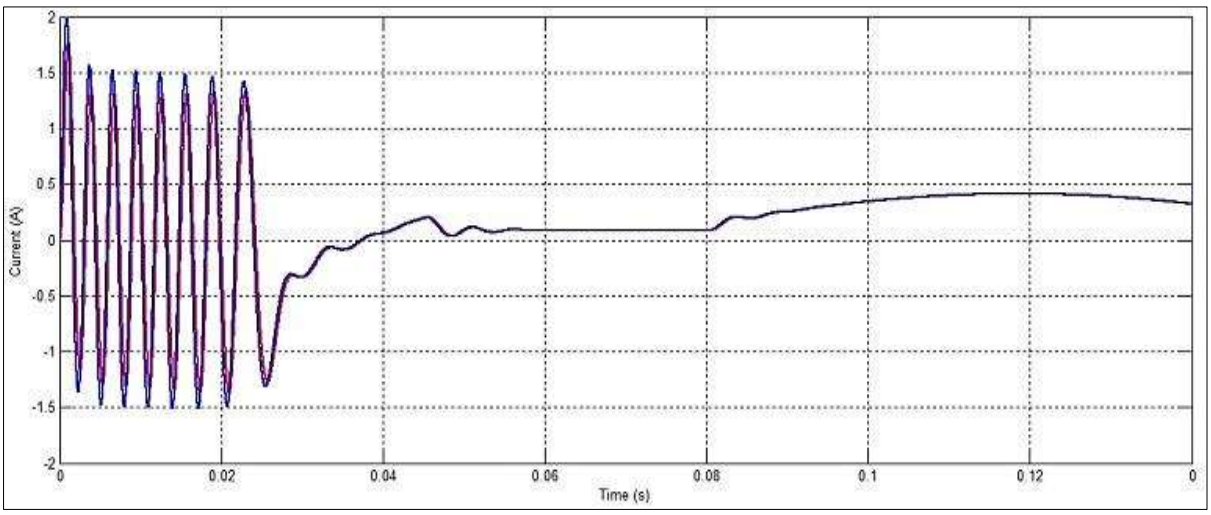

Fig. 12. *Estimated (Red) and Real (Blue) IQS (A) Under Variable Load Condition.*

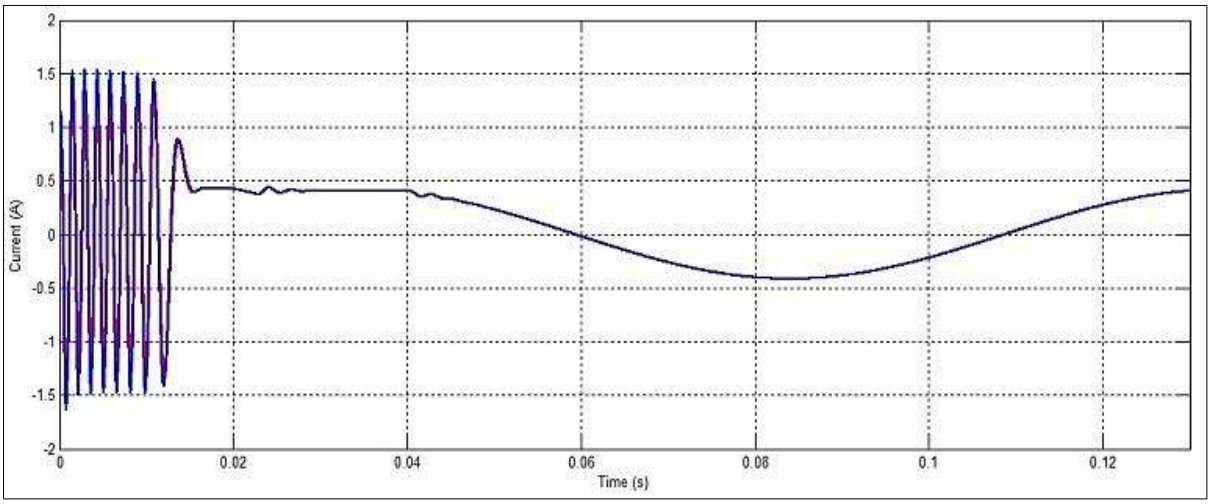

Fig. 13: *Estimated (Red) and Real (Blue)* i_{ds} *(A) Under Variable Load Condition.*

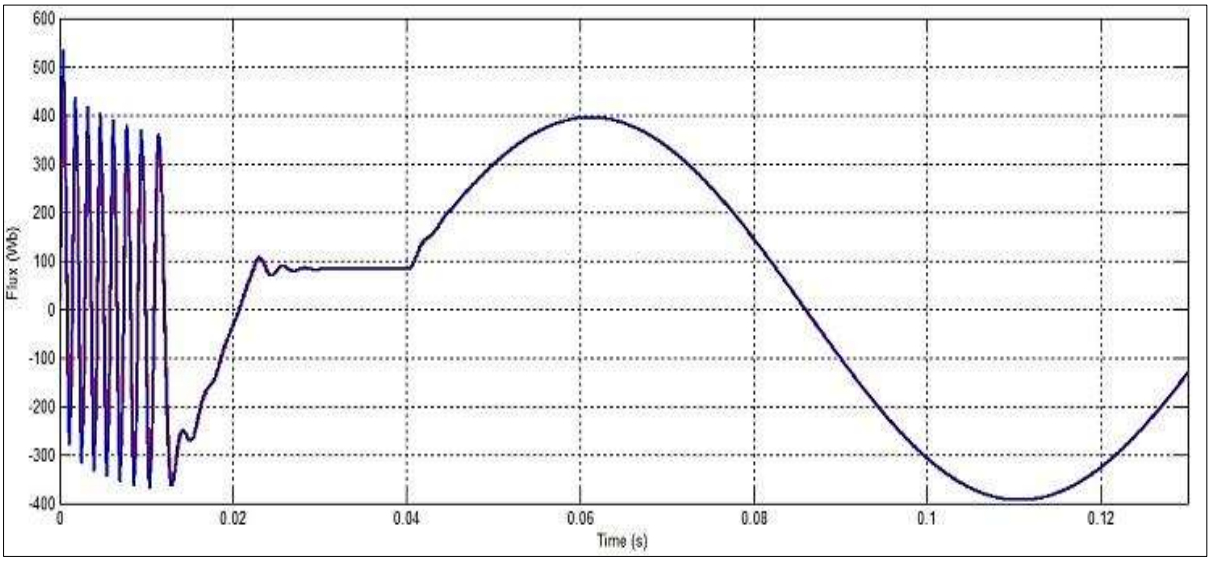

Fig. 14: *Estimated (Red) and Real (Blue)* λ'_{qr} (Wb) *Under Variable Load Condition.*

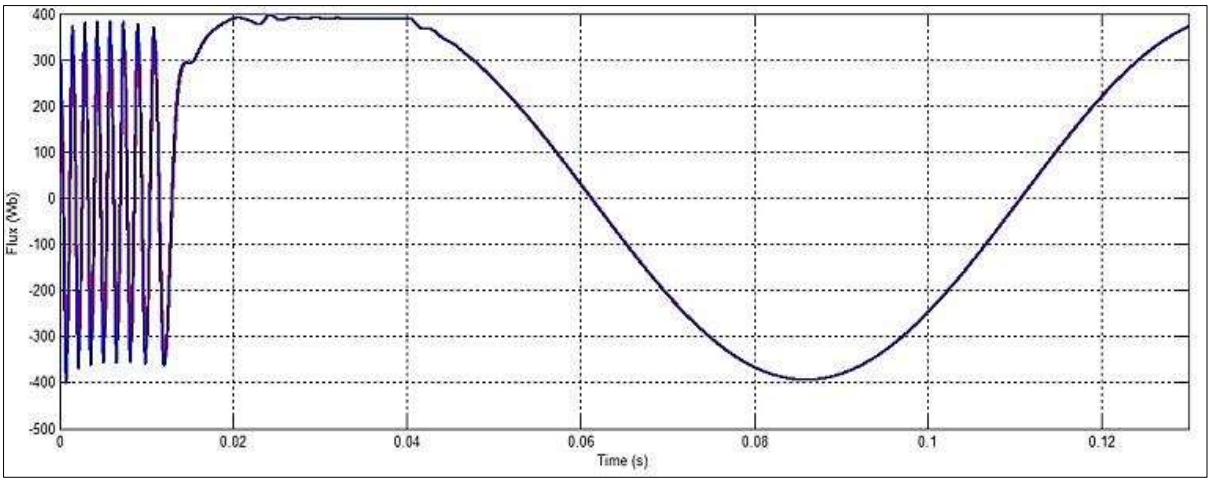

Fig. 15: *Estimated (Red) and Real (Blue)* λ'_{dr} (Wb) *Under Variable Load Condition.*

To verify the prominence of EKF rather than other proposed estimators for hysteresis motor, the results of EKF estimator are compared by the presented results using a model reference adaptive system (MRAS) estimator [13]. Figure 16 shows the general block diagram used for this purpose. In Figure 17, speed estimation is shown using MRAS at no-load condition. Due to some oscillations of estimated speed, it is clear that the transient performance of EKF estimator is better than MRAS estimator.

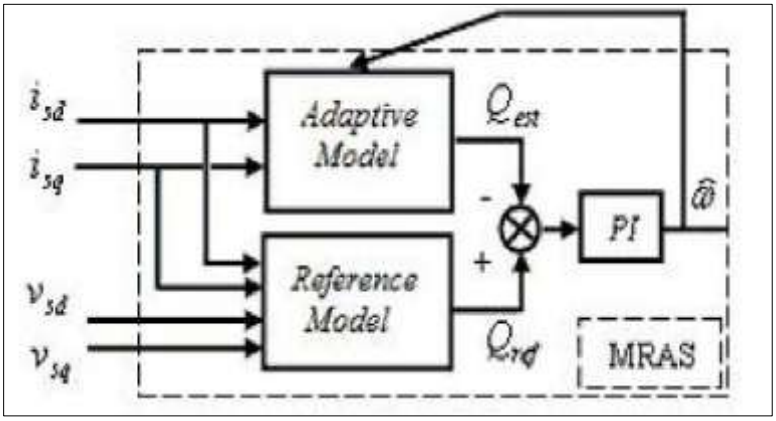

Fig. 16: *Block Diagram of MRAS Estimator [13].*

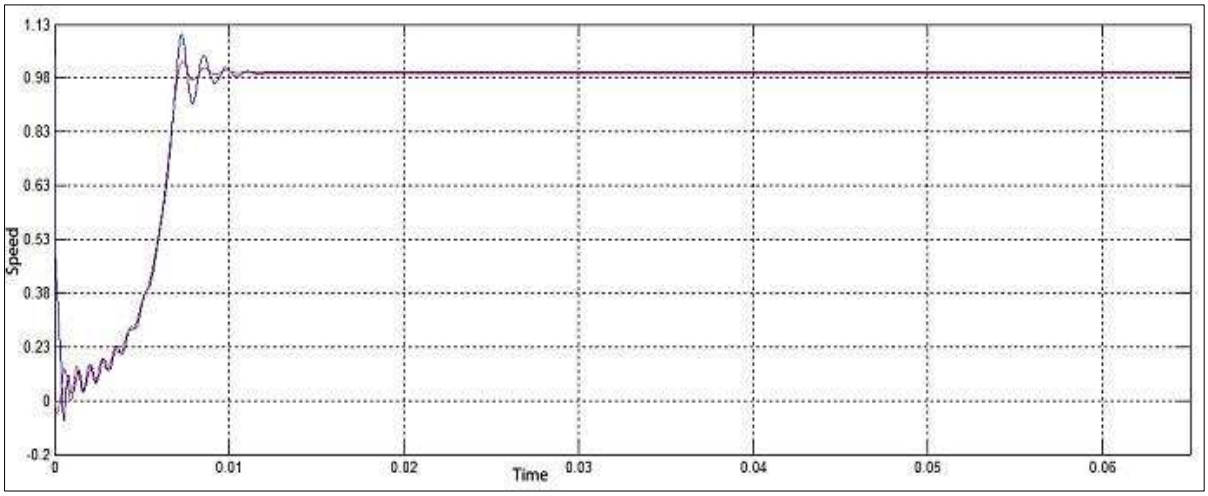

Fig. 17: *Real Speed (Blue) And Estimated Speed With MRAS (Red) At No Load.*

CONCLUSION

In this study, a new approach for speed estimation of hysteresis motor based on extended kalman filter (EKF) has been presented. The filtering action of EKF improves the system performance. Simulation results reveal that the state variables and speed tracking are good and error convergence is guaranteed.

They validate the performance of proposed method under constant or variable load torque and also in synchronous or asynchronous regions. Also, the performance of EKF estimator has been compared with MRAS estimator and it has been shown that speed estimation with MRAS in transient time is not so accurate than speed estimation with EKF. Developed estimation system can be used for closed-loop control of hysteresis motor via scalar of vector control strategies.

REFERENCES

1. Roters CH. The hysteresis motor-advances which permit economical fractional horsepower ratings. *Trans. of the American Institute of Electrical Engineers*. 1947; 66(1): 1419–1430p.
2. Copeland MA, Slemon GR. An analysis of the hysteresis motor: part-II-then circumferential-flux machine. *IEEE Trans. on Power Apparatus and Systems*. Jun 1964; 83: 619–625p.
3. Tadakuma S, Tanaka S, Inahaki J et al. Hysteresis Motors Controlled by Inverters. *Electrical Engineering in Japan*. 1972; 96(2): 88–`96p
4. Rabbi et al. Modeling and V/F control of a Hysteresis Interior Permanent Magnet Motor. *IEEE International Advance Computing Conference (IACC)*. 2014; 1–8p.
5. Qian J, Rahman MA. Analysis of Field Oriented Control for Permanent Magnet Hysteresis Synchronous Motor. *IEEE Trans. on Industry Application*. Nov 1993; 29(6): 1156–1163p.
6. Zare M, Niasar AH. A Novel Sensorless Vector Control of Hysteresis Motor Drive. *In Proceedings of the 4th IEEE Power Electronics, Drive Systems & Technologies Conference* (PEDSTC). 2013; 261–264p.
7. Peter V. Sensorless Vector Control and Direct Torque Control. *Oxford.* 1998.
8. Smidl V, Peroutka Z. Advantages of Square-Root Extended Kalman Filter for Sensorless Control of AC Drives. *IEEE Trans. on Industrial Electronics*. 2012; 59(11): 4189–4196p.
9. Bolognani S, Tubiana L, Zigliotto M et al. Extended Kalman filter tuning in sensorless PMSM drives. *IEEE Trans. on Industry Applications*. 2003; 39(6): 1741–1747p.
10. Slemon GR, Jackson RD, Rahman MA et al. Performance Prediction for Large Hysteresis Motors. *IEEE Trans. on Power Apparatus and Systems*. Nov./Dec 1977; PAS-96(6): 1915–1919p.
11. Rahman MA. Analytical Models for Poly Phase Hysteresis Motor. *IEEE Trans. on Power Apparatus and Systems*. 1973; PAS-92(1): 237–242p.
12. Badeeb OM. Investigation of the Dynamic Performance of Hysteresis Motors using MATLAB/SIMULINK. *Journal of Electrical Engineering*. 2005; 56(3–4): 106-109p.
13. Niasar AH, Zare M, Moghbelli H. Dynamic Modeling and Simulation of a Super-High-Speed Circumferential-Flux Hysteresis Motor. *Journal of Engineering*. 2013; Article ID 898634, 1–7p.
14. Nitao J, Scharlemann ET, Kirkendall BA et al. Equivalent Circuit Modeling of Hysteresis Motors. *U.S. Department of Energy by Lawrence Livermore National Laboratory*. Report no. LLNL-TR-416493, Jul 2009.
15. Qian J, Rahman MA. Analysis of Field Oriented Control for Permanent Magnet Hysteresis Synchronous Motor. *IEEE Trans. on Industry Application*. 1993; 29(6): 1156–1163p.
16. Darabi et al. Dynamic Performance Analysis of Hysteresis Motors by a Linear Time-Varying Model. *Iranian Journal of Electrical & Electronic Engineering*. 2008; 4(4): 202–215p.
17. Shi et al. Speed estimation of an induction motor drive using an optimized extended Kalman filter. *IEEE Trans. Ind. Electronics*. Feb 2002; 49(1): 124–133p.

18. Leite AV, Araujo RE, Freitas D et al. Full and reduced order extended kalman filter for speed estimation in induction motor drives. *35th Annual IEEE Power Electronics Specialists Conference*. 2004; (3): 2293–2299p.

Cite this Article
AH. Niasar, AN. Darbaghshahi, M. Shirani. Speed Estimation of High-Speed Hysteresis Motor Based on Extended Kalman Filter. *Journal of Power Electronics and Power Systems.* 2016; 6(1):